

Wind Tunnel Calibration Procedures

Zakary Steenhoek

This experiment aimed to calibrate a pressure transducer and a scannivalve in a low-speed wind tunnel and to determine the airflow velocity in the test section as a function of fan speed. Calibration curves for the pressure transducer and scannivalve were developed by comparing their digital readings with those from a manometer. Using Bernoulli's equation and mass conservation principles, pressure and velocity relationships were evaluated across a range of fan settings for each instrument. The results show a linear relationship with minimal deviation from the true flow speed. This calibration procedure confirmed the effectiveness of the instruments and laid baseline measurements for an empty test section for future aerodynamic experiments.

I. Nomenclature

ρ	=	air density
Ψ	=	volume
n	=	molar mass
R	=	universal gas constant
T	=	temperature
U	=	internal energy
KE	=	kinetic energy
PE	=	potential energy
$C\Psi$	=	control volume
CS	=	control surface
\hat{n}	=	normal vector
∂	=	partial derivative
M	=	conversion factor
E	=	voltage
p_{static}	=	static pressure
p_{total}	=	total pressure
p_{gauge}	=	gauge pressure
p_{MM}	=	manometer pressure
V_{∞}	=	dynamic velocity
\dot{m}	=	mass time derivative
A_1	=	upstream cross-sectional area
A_2	=	downstream cross-sectional area
f	=	fan speed
p_1	=	upstream static pressure <i>tmp</i>
p_2	=	downstream static pressure <i>tmp</i>
δP	=	differential pressure across the test section <i>tmp</i>
P_{atm}	=	absolute atmospheric pressure (<i>kPa</i>)
V_1	=	upstream flow velocity <i>tmp</i>
V_1	=	downstream flow velocity <i>tmp</i>

II. Introduction

Calibration of measurement instruments is crucial for accurate data collection in any engineering experimentation. The purpose of this experiment is to calibrate the machines used to determine air flow velocity through the test section of a wind tunnel. The machines in question include a pressure transducer, a scannivalve, and a manometer. The low-speed wind tunnel in question operates across multiple fan settings, and provides an ideal environment to study the pressure-velocity relationship using Bernoulli's principle and mass conservation.

A. Objective

The goal of this test is first to determine the laboratory air density. This provides an important starting point, from which flow velocity can be determined as a function of pressure. Before that can be done, however, pressure must be measured in some meaningful way, which is the next goal of this experiment. More specifically, how well the digital pressure transducer and scannivalve readings correspond to the analog manometer reading. The final objective is to use these pressure measurements to determine the flow velocity inside the empty test section of a low-speed wind tunnel using the calculated laboratory air density. An understanding of these instruments and how each of them record data is important, and calibration ensures reliability and provides a baseline for future experimentation.

B. Assumptions

Assumptions are made in this experiment which make it possible to produce meaningful results without creating substantial error. These assumptions allow for simplicity in data collection and processing, and allow the use of some key physical laws. Assumptions made include the following:

1. Ideal Atmosphere

To determine the density of the laboratory air, the ideal gas law is used, which is only applicable to ideal gasses. The assumption is made that the atmosphere may be treated as an ideal gas.

2. Incompressible & Uniform Flow

Methods to determine flow velocity through the test area apply the conservation of mass. The fluid flow is assumed to be uniform, and density of laboratory air is assumed to be constant, and therefore the term representing the change in mass inside the control volume w.r.t time evaluates to zero.

3. Inviscid Fluid

Methods to determine flow velocity through the test area apply the conservation of energy. The effects of viscous forces on the fluid are assumed to be negligible, and therefore energy loss can be neglected, and Bernoulli's equation may be applied.

C. Physical Laws

1. Ideal Gas Law

The first governing law in this experiment fundamental ideal gas law, Eq. (1). This is a thermodynamic equation of state for an ideal gas, which relates physical properties and known constants.

$$pV = nRT \quad (1)$$

2. Bernoulli's Equation

The next governing law is the fundamental conservation of energy equation, Eq. (2), which states that the total energy of a system, consisting of the internal energy U , the kinetic energy KE , and the potential energy PE , remains constant.

$$U + KE + PE = \text{const.} \quad (2)$$

3. Mass Conservation

The next governing law is the fundamental conservation of mass, Eq. (3), which states that the change in mass inside a control volume w.r.t time plus the mass convected across the control surface must always sum to 0.

$$\frac{\partial}{\partial t} \int_{CV} \rho \, dV + \int_{CS} \rho (\vec{V} \cdot \hat{n}) \, dA = 0 \quad (3)$$

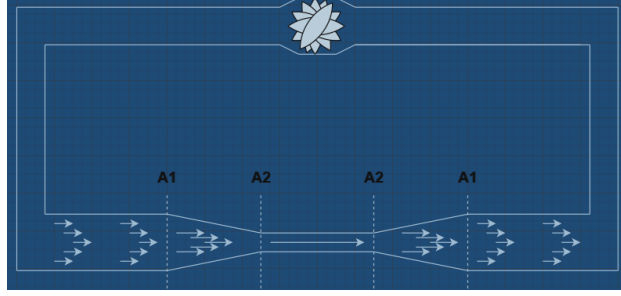


Fig. 1 General wind tunnel setup. Note the contraction area on the left-hand side, where the cross-sectional area reduces from A_1 to A_2 .

4. Error Propagation

The final governing equation is Gauss's formula for error propagation, Eq.(4), which describes the effect of uncertainty in a calculation as a function of the uncertainty in the variables involved, where i is the number of variables with uncertainty.

$$\delta y = \sqrt{\sum_i \left(\frac{\partial y}{\partial x_i} \delta x_i \right)^2} \quad (4)$$

D. Experimental Equipment

1. Low-speed wind tunnel

A low speed wind tunnel[1] is a large lab machine with a fan, flow normalization, a test section, and related instrumentation. The tunnel used in this experiment is a closed tunnel, which circulates a constant volume of air through a ducting system using a fan. Before the test section, the cross-sectional area of the tunnel decreases, and according to Eq.(3), the velocity must increase. This closed system creates an optimal environment for aerodynamic testing. A general wind tunnel diagram is shown in Fig.1

2. Absolute pressure transducer

An absolute pressure transducer[2] is a digital measurement device that measures pressure in the absolute range, i.e. from a zero-reference point, displayed in kilopascals. It works by generating a voltage difference between the measurement side, exposed to the atmosphere, and the non-measurement side, which is exposed to a permanently sealed, near-perfect vacuum. This measurement is integral to determining the density of the atmosphere inside of the lab.

3. Digital thermocouple

A digital thermocouple[3] is a digital measurement device that measures temperature, displayed in degrees Celsius. The device consists of two conductors of different metals - the hot and the cold junction. When the hot junction is heated, it generates a voltage proportional to the temperature difference between the plates. This measurement is integral to determining the density of the atmosphere inside of the lab.

4. Pressure transducer

The pressure transducer works in a similar way to the absolute pressure transducer described above, but measures the difference between two pressure values, and writes a proportional output in volts. One side of this device reads the stagnation pressure, while the other side reads the static pressure. The measurement obtained from this device is a gauge pressure.

5. Micro-manometer

A micro-manometer[4] is an analog measurement device used to measure pressure, displayed in inches of water. It operates on the principal of hydrostatic equilibrium, which states that the pressure exerted by a column of fluid is

proportional to its height and density. The pressure being measured causes a column of water to rise to fall in a clear tube. Once equilibrium is reached and the meniscus is centered between the inscribed lines, a measurement of static gauge pressure drop across the contraction may be taken.

6. Scannivalve

A Scannivalve[5] is a digital measurement device similar to the transducer, and is used to measure pressure at multiple different locations, or 'ports'. It consists of a single transducer and a mechanism that switches the port as needed. This allows for smaller error, as a single machine can read at multiple different points. This measurement provides gauge pressure at several points across the test section.

7. Pitot tube

A pitot tube[6] is a physical tube-shape object with a central hole down the length of the tube and several holes drilled around the outside of the tube. These holes are kept separate, and the pressure transducer is connected across these holes to read the difference, i.e. the dynamic pressure. This is the device connected to the pressure transducer. There is a 90 degree bend present to normalize any disrupting airflow inside the tube.

III. Procedure

A. Data Collection

1. Part 1: Ambient Air Density

For the first part of the data collection, the ambient air density must be determined. This is done by taking measurements of the absolute pressure and the temperature inside the wind tunnel, using the absolute pressure transducer and digital thermocouple, respectively. The governing equation here is the fundamental ideal gas law, Eq.(1), which relates pressure, volume, temperature, matter, and the universal gas constant. This equation can be rearranged and simplified by expanding the term representing matter into m/M , introducing density as m/V , and defining the specific gas constant as R/M as seen in Eq.(5).

$$p = \frac{m}{V} \frac{R}{M} T \quad (5)$$

The result is Eq.(6), which relates pressure, density, and temperature with a known constant value specific to air.

$$p = \rho RT \quad (6)$$

This equation can then rearranged to solve for ρ as a function of p and T , seen in Eq.(7).

$$\rho = \frac{p}{RT} \quad (7)$$

This is the numerical value for density to be used henceforth in this experiment. The error associated with this measurement is found using Eq.(8), derived from Eq.(4), the partial derivatives of Eq.(7) w.r.t. p and T , and the known machine errors, δp and δT .

$$\delta \rho = \sqrt{\left(\frac{1}{RT} \delta p\right)^2 + \left(\frac{p}{RT^2} \delta T\right)^2} \quad (8)$$

2. Part 2: Instrument Calibration

For the second part of the data collection, connect the manometer, scannivalve, and pressure transducer inline with each other to the pitot tube inside the test section. This configuration records pressure data from each instrument relative to the others. This data is used to find the calibration curves for the digital pressure readings produced from the scannivalve and pressure transducer, relative to the analog reading from the micro-manometer. Record the manometer reading, the scannivalve voltage, and the pressure transducer voltage at the following fan speeds: 15, 20, 25, 30, 35, 40, 45, and 50 Hz. Be sure to include the provided manometer bias to *all* manometer measurements. Compute a least-squares linear regression for the scannivalve and the pressure transducer, Eq.(9), with the manometer pressure as the ordinate and the scannivalve and pressure transducer voltage as the abscissa. Record the coefficient M for the

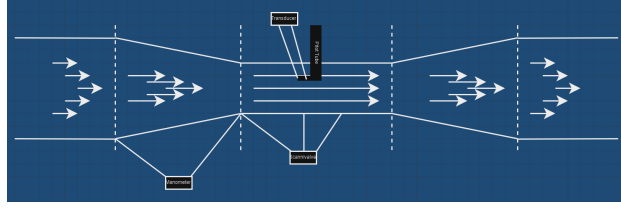


Fig. 2 Part 3 measurement configuration. Note that this is a zoomed version of Fig. 1. Also note that the instrument configuration is different in part 2.

linear term of each regression line. This is the conversion factor for the scannivalve & transducer pressure in volts and pressure in pascals. *Note that the variable E is used for voltage to differentiate it from velocity.*

$$p = ME + b \quad (9)$$

The error associated with this conversion factor can be derived from Eq. (4). Since the data collected is numerical, and Eq. (9) contains only one variable with uncertainty, Eq. (10) is found.

$$\delta p = \sqrt{\sum_{i=0}^n \left(\frac{\partial p}{\partial E_i} \delta E_i \right)^2} \quad (10)$$

The caveat here is that the machine error for every measurement taken is the same, allowing this to be simplified greatly, yielding Eq. (11).

$$\delta p = \sqrt{\left(\frac{\partial p}{\partial E} \delta E \right)^2} = \frac{\partial p}{\partial E} \delta E \quad (11)$$

Finally, note that the partial derivative of p w.r.t E is just the conversion factor M , and the final equation for conversion factor error, Eq. (12), is found as a factor of the scannivalve and pressure transducer machine error.

$$\delta p = M \delta E \quad (12)$$

3. Part 3: Wind Tunnel Calibration

For the third part of the data collection, the instrument configuration is modified such that each machine records pressure data independently. The manometer is connected across the wind tunnel's contraction area, and records the static pressure drop. The pressure transducer is connected across the pitot tube, and records dynamic pressure at the center line of the test section. The scannivalve is connected to several ports in the floor of the test section - one at the entry, one near the center, and one toward the back - to measure the gauge pressure at different points across the test section. This data is used to find the velocity curve for each machine with an empty test section. This configuration can be seen in Fig. 1.

Record the manometer reading, the scannivalve voltage, and the pressure transducer voltage at the following fan speeds: 15, 20, 25, 30, 35, 40, 45, and 50 Hz. Be sure to include the provided manometer bias to *all* manometer measurements. Using the conversion factors obtained in part 2, find the pressure recorded by the scannivalve and the pressure transducer. The velocity in the test section can now be found using the pressure readings from the three different instruments. For the scannivalve and pressure transducer, this can be done using Bernoulli's equation (13), a derivation of Eq. (2). Details of this derivation will not be presented in this report, however it should be noted that the Bernoulli equation only holds when the fluid is considered to be incompressible with negligible viscous effects, and is in the absence of any significant external forces.

$$p_0 + \frac{1}{2} \rho V^2 + \rho g z = \text{const.} \quad (13)$$

The term representing hydrostatic fluid pressure, $\rho g z$, can be neglected for this analysis, as the pressure contribution from the weight of the air is negligible. This produces Eq. (14), equating the total pressure, i.e. p_{abs} to the sum of the static pressure, i.e. P_{atm} , and the dynamic pressure, i.e. $\frac{1}{2} \rho V_{\infty}^2$.

$$p_{total} = p_{static} + \frac{1}{2} \rho V_{\infty}^2 \quad (14)$$

Note the similarity between this equation and the definition of gauge pressure, $p_{abs} = p_{atm} + p_{gauge}$, or $p_{gauge} = p_{abs} - p_{atm}$. Applying this and rearranging Eq. (14) to solve for V_{∞} produces Eq. (15), which can be used to find velocity as a function of pressure and density.

$$V_{\infty} = \sqrt{\frac{2 \cdot p_{gauge}}{\rho}} \quad (15)$$

The error in this measurement, Eq., can be derived from Eq. (4) as a function of the partial derivatives of V_{∞} w.r.t. p_{gauge} and ρ , and their respective uncertainty values, δp_{gauge} and $\delta \rho$. *Note that the data collected is numerical, similar to Eq. (10), but since the uncertainty in both variables is constant throughout the data collection, this simplification was skipped.*

$$\delta V_{\infty} = \sqrt{\left(\frac{\partial V_{\infty}}{\partial p_{gauge}} \delta p_{gauge}\right)^2 + \left(\frac{\partial V_{\infty}}{\partial \rho} \delta \rho\right)^2} \quad (16)$$

For the micro-manometer, the velocity is derived using a combination of Bernoulli's equation and mass conservation, Eq. (3). One of the working assumptions states incompressibility, which allows ρ to be treated as a constant. This assumption greatly simplifies Eq. (3), and produces Eq. (17).

$$\rho \int_{CS} (\vec{V}_{\infty} \cdot \hat{n}) dA = 0 \quad (17)$$

This assumption also states uniform flow, and since the two cross-sectional areas of the wind tunnel in question are planar in nature and mass cannot phase through the solid walls of the wind tunnel, $(\vec{V}_{\infty} \cdot \hat{n})$ is simply the velocity into and out of the contraction area. This yields Eq. (18).

$$\rho \int_{A_1}^{A_2} \vec{V}_{\infty} dA = 0 \quad (18)$$

This integral can be evaluated to produce Eq. (19), which states that the rate of change of mass w.r.t is equal to the density times the area times the velocity.

$$\dot{m} = \rho A_1 \vec{V}_1 = \rho A_2 \vec{V}_2 \quad (19)$$

Since density is present on both sides, dividing Eq. (19) by density and rearranging to solve for V_1 finally produces a simple equation relating the areas and velocities at the contraction area boundaries, seen in Eq. (20).

$$\vec{V}_1 = \vec{V}_2 \frac{A_2}{A_1} \quad (20)$$

This can be used in conjunction with a rearranged Bernoulli's equation to determine the velocity at each contraction area boundary, since the ratio $\frac{A_2}{A_1}$ is a known quantity. Here, the term representing hydrostatic fluid pressure, $\rho g z$, can still be neglected. Since this is equal to a constant, Eq. (21), similar to Eq. (19), is derived, relating differential pressure to differential velocity.

$$p_1 - p_2 = \frac{1}{2} \rho (\vec{V}_2^2 - \vec{V}_1^2) \quad (21)$$

The manometer measures this differential pressure across the contraction area, and as such, the only unknown variables are \vec{V}_1 and \vec{V}_2 . The system of equations, Eq. (20) & Eq. (21) can be solved to find the velocity at the entry to the test area. Substituting Eq. (20) into Eq. (21) and rearranging, the final equation for \vec{V}_2 is found in Eq. (22). *Note ($p_1 - p_2$) was rewritten as p_{MM}*

$$\vec{V}_2 = \sqrt{\frac{2(p_{MM})}{\rho(1 - \frac{A_2}{A_1})}} \quad (22)$$

The error associated with this conversion factor, Eq. (23), can be derived from Eq. (4). *Note that the data collected is numerical, similar to Eq. (10), but since the uncertainty in both variables is constant throughout the data collection, this simplification was skipped.*

$$\delta \vec{V}_2 = \sqrt{\left(\frac{\partial \vec{V}_2}{\partial p_{MM}} \delta p_{MM}\right)^2 + \left(\frac{\partial \vec{V}_2}{\partial \rho} \delta \rho\right)^2} \quad (23)$$

This equation is used to solve for the error in the measured manometer velocity as a function of the partial derivatives of \bar{V}_2 w.r.t p_{MM} and ρ , and their respective uncertainty values, δp_{MM} and $\delta \rho$.

Compute the velocity as a function of the pressure measurements from all three instruments using the relevant equations derived above. Compute a least-squares linear regression for each with the velocity as the ordinate and the fan speed as the abscissa. Record the linear coefficient for each regression line. These are the calibration curves that relate flow velocity as measured by each instrument to the speed of the fan.

B. Data Processing

Declare all global variables, including R_{air} , the manometer bias, the provided machine errors, the contraction area ratio, and symbolic variables P , T , MM , and RHO . Define anonymous functions for Eq. (7), Eq. (15), and Eq. (22) using these symbolic variables. Import the data from the files using `importdata()` and extract the needed columns. Also define anonymous functions for the conversion between inches of water and pascals (7). *Be sure to also convert the manometer error to pascals.*

1. Part 1: Ambient Air Density

Use the defined function for the ideal gas law to compute ρ . Take the partial derivative of this function w.r.t. both p and T using the `diff()` command. This will evaluate the partial derivatives symbolically, which is then used to calculate the numerical values. Compute the error using Eq. (8).

2. Part 2: Instrument Calibration

To find the linear regression coefficients for part 2, the `polyfit()` command is used on the vectors, passing in the scannivalve and pressure transducer readings and specifying a first order least-squares regression. Extract the linear coefficient M for each regression and multiply this by the corresponding machine error, as seen in Eq. (12), to find δp_{sv} and δp_{pt} . Graph the manometer pressure as a function of scannivalve and transducer voltage. Using `fplot(poly2sym(<coefficient_vector>))`, the coefficients returned from `polyfit()` are turned into a symbolic equation and displayed on the graph. Include error bars using `errorbar()` and the relevant uncertainties.

3. Part 3: Wind Tunnel Calibration

Determine the scannivalve and transducer pressure measurements by multiplying the vectors containing the voltage readings by their respective conversion factors from part 2, as seen in Eq. (9). Using these pressure values, use the defined function for dynamic velocity to determine the velocity as a function of pressure and density, as seen in Eq. (15). Compute the least-squares linear regression, passing in the fan speed and instrument velocities. Compute the error in these velocities by determining the symbolic derivatives w.r.t. p and ρ , evaluating them with the numerical data, and computing Eq. (16). A similar approach is used to determine V_2 from the manometer readings. Use the anonymous function for Eq. (22), compute the least-squares linear regression, passing in fan speed and manometer velocity, and use Eq. (23) to determine the manometer velocity error. Finally, compute the least-squares linear regression on the true velocity from part 3. This procedure yields linear regressions for velocity, as measured by all three instruments, and the true measured velocity. The same methods described in part 2 are used to plot velocity as a function of fan speed for each measurement device, including the error bars. Finally, these velocities are all plotted on a single figure with the true velocity, allowing a visual interpretation of the derived machine velocity in comparison with the true velocity.

IV. Results

Raw data used for these calculations can be found in [8] [9]. The air density inside the wind tunnel was calculated based on the measured temperature T of $32.7^\circ\text{C} = 305.85\text{K}$ [10] and measured p_{atm} of 96.29 kPa , yielding a value of 1.0970 kg/m^3 with an uncertainty of 0.0038 kg/m^3 . The least-squares linear regression calibration curves for the pressure transducer and scannivalve readings against the manometer readings, from Tbl. 1, are shown in Fig 3 and Fig 4, respectively. The scannivalve had a calibration slope M of 496.1171 Pa/E , while the pressure transducer had a calibration slope M of 1335.041 Pa/E . Note that the recorded scannivalve voltages were negative, so the absolute value of these readings were taken for consistency.

The figures seen above, Fig 3 and Fig 4, show a very accurate linear relationship between the manometer reading and the scannivalve & pressure transducer voltages. This can be deduced by just a simple visual analysis of these figures,

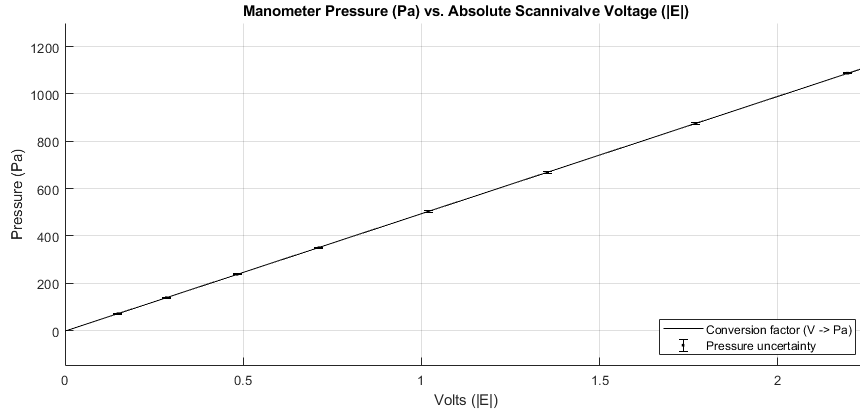


Fig. 3 Manometer pressure plotted against the voltage readout from the scannivalve. *Note the small error and linearity of the LSQ fit*

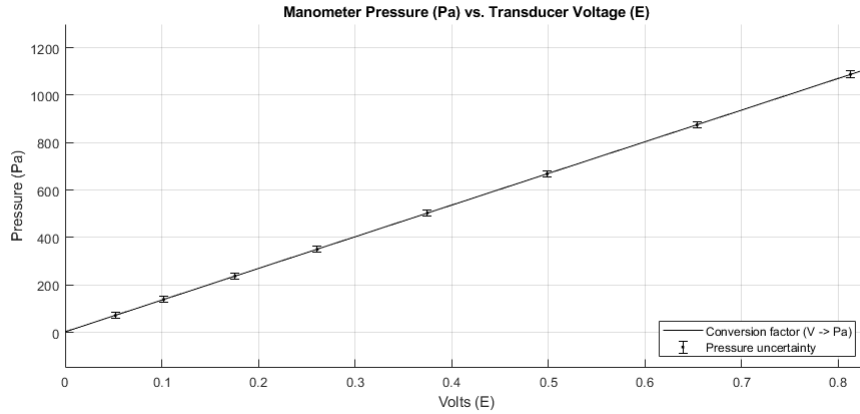


Fig. 4 Manometer pressure plotted against the voltage readout from the pressure transducer. *Note the small error and linearity of the LSQ fit*

but calculating the R^2 values for both proves the linearity of the data, as the R^2 for both regressions returns exactly 1.0000. The associated pressure uncertainty for the scannivalve was 2.4806 Pa, and the associated pressure uncertainty for the pressure transducer was 13.3504 Pa. The machine error in the manometer reading converted to pascals was 1.2454 Pa [7]. The M values were used to find the pressure recorded by each machine. This data is tabulated in Tbl.4. Then the velocity measured by the scannivalve and pressure transducer was computed. This data is tabulated in Tbl.6. The least-squares linear regression calibration curves for the scannivalve and pressure transducer velocity against the fan speed are shown in Fig 5 and Fig 6 respectively. The Scannivalve had a calibration slope of $0.8872 \frac{m/s}{Hz}$ and the pressure transducer had a calibration slope of $0.9551 \frac{m/s}{Hz}$. The related uncertainty in these measurements can be seen in table .

The velocity at A_2 was computed using the manometer readings. This data is tabulated in Tbl.6. The least-squares linear regression calibration curves for the manometer velocity against the fan speed is shown in Fig 7. The manometer had a calibration slope of $0.9355 \frac{m/s}{Hz}$. The related uncertainty in these measurements can be seen in table .

The velocity calibration curves for all three instruments were finally plotted with the least-squares linear regression curve for the true velocity against the fan speed, as seen in Fig 8. The true velocity data can be seen in Tbl.2.

Once again, a simple visual analysis of Fig 8 shows that the calculated flow speed from all three measurement devices has very small amounts of deviation from the true flow speed. The four regressions plotted here overlap nearly entirely in the 15 - 20 Hz range, and the deviations after that are marginal. Note that there are actually four curves in the Fig 8 but the curves for the true velocity and the pressure transducer overlap entirely across the extent of the fan frequency range.

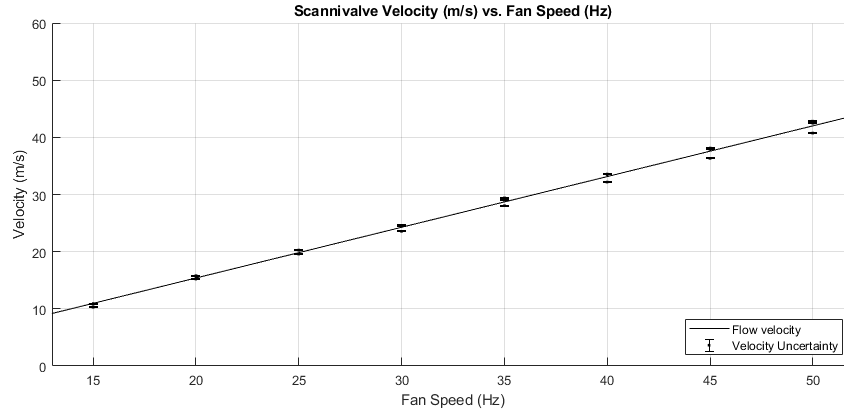


Fig. 5 Manometer pressure vs. scannivalve and pressure transducer voltage

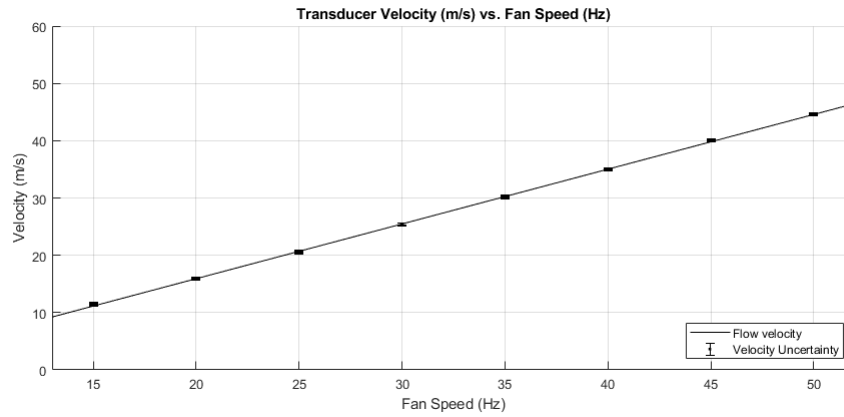


Fig. 6 Manometer pressure vs. scannivalve and pressure transducer voltage

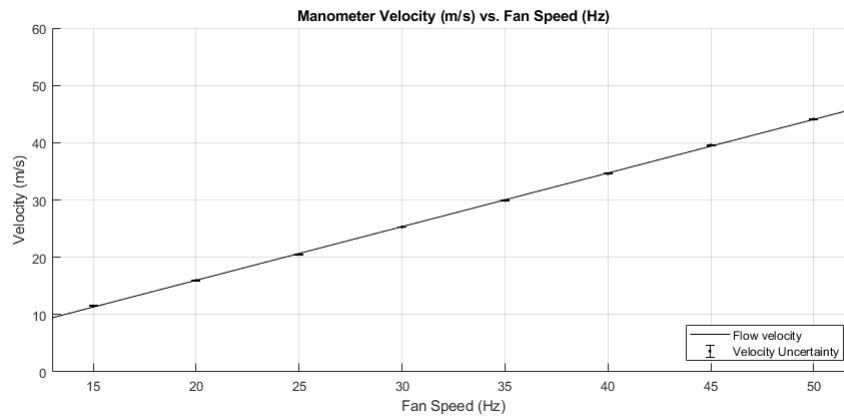


Fig. 7 Manometer pressure vs. scannivalve and pressure transducer voltage

V. Conclusion

The experiment successfully met the objective of calibrating the pressure transducer and scannivalve and confirmed the linear behavior with respect to manometer readings. The results showed that both instruments can reliably measure pressure and velocity within the wind tunnel, as long as the machine errors and uncertainty propagation is carried through. The results also showed that the airflow speed increases linearly with fan frequency, which validates the wind

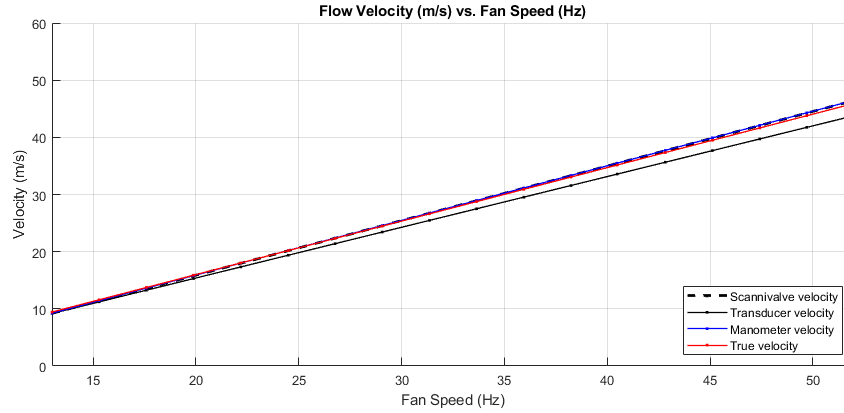


Fig. 8 Manometer pressure vs. scannivalve and pressure transducer voltage

tunnel and instrument setup for future testing. The assumptions made prior to experimentation are crucial to obtaining any sort of meaningful calibration. They allow for a simpler derivation of pressure and velocity using physical laws like the conservation of mass and Bernoulli's equation, which may not apply without these working assumptions. The results of the experiment show that these assumptions had next to no negative affect on the measurements, as each instrument measures the pressure and velocity with great accuracy in comparison to the true velocity. The results do meet the expectations, as linear slopes were obtained that relate the digital readings to physical properties of the flow. These can be applied in the future as a baseline measurement of flow in an empty test section, which could be used to measure the difference in physical properties when the test section has an object inside. The error associated with this experiment was found to be very small. One obvious way to reduce this error is to use more precise and accurate measurement instruments, however this would yield results that are not much different. Another way to reduce error would be to be more careful when taking the manometer readings in part 2, as this would relate the digital scannivalve and pressure transducer more closely to the real pressure differential present across the test section.

I. Appendix A: Tabulated Data

Table 1 Raw Wind Tunnel Data (Part 2)

Wind Tunnel Setting (Hz)	Air Temp. (°C)	Manometer (in H ₂ O)	Pressure Transducer (E)	Scannivalve Reading (E)	Scannivalve Port #	Velocity (m/s)	Ambient Pressure (kPa)
15.000	32.315	0.238	0.052	-0.148	1.000	11.281	96.290
20.000	31.337	0.510	0.102	-0.284	1.000	15.748	96.290
25.000	31.846	0.905	0.176	-0.483	1.000	20.569	96.290
30.000	31.028	1.358	0.261	-0.712	1.000	25.115	96.290
35.000	32.074	1.973	0.375	-1.019	1.000	30.128	96.290
40.000	31.631	2.635	0.499	-1.354	1.000	34.762	96.290
45.000	29.993	3.464	0.654	-1.769	1.000	39.671	96.290
50.000	33.635	4.320	0.813	-2.196	1.000	44.518	96.290

Table 2 Raw Wind Tunnel Data (Part 3)

Wind Tunnel Setting (Hz)	Air Temp. (°C)	Manometer (in H ₂ O)	Pressure Transducer (E)	Scannivalve Reading (E)	Scannivalve Port #	Velocity (m/s)	Ambient Pressure (kPa)
15.000	31.206	0.236	0.053	0.132	0.000	11.323	96.290
15.000	31.274	0.236	0.053	0.129	1.000	11.289	96.290
15.000	31.354	0.236	0.054	0.117	2.000	11.405	96.290
20.000	32.697	0.500	0.104	0.256	0.000	15.906	96.290
20.000	32.717	0.500	0.104	0.276	1.000	15.893	96.290
20.000	32.761	0.500	0.104	0.272	2.000	15.933	96.290
25.000	31.447	0.855	0.174	0.424	0.000	20.533	96.290
25.000	31.168	0.855	0.173	0.455	1.000	20.516	96.290
25.000	30.988	0.855	0.174	0.454	2.000	20.456	96.290
30.000	32.384	1.324	0.263	0.614	0.000	25.317	96.290
30.000	32.428	1.324	0.263	0.669	1.000	25.319	96.290
30.000	32.471	1.324	0.263	0.660	2.000	25.339	96.290
35.000	32.048	1.872	0.372	0.870	0.000	29.963	96.290
35.000	31.856	1.872	0.374	0.955	1.000	30.007	96.290
35.000	31.721	1.872	0.371	0.933	2.000	30.030	96.290
40.000	33.979	2.522	0.503	1.144	0.000	35.008	96.290
40.000	34.061	2.522	0.501	1.247	1.000	34.993	96.290
40.000	33.973	2.522	0.503	1.240	2.000	35.033	96.290
45.000	31.292	3.312	0.657	1.460	0.000	39.891	96.290
45.000	31.449	3.312	0.657	1.607	1.000	39.889	96.290
45.000	31.585	3.312	0.658	1.589	2.000	39.894	96.290
50.000	32.688	4.122	0.818	1.835	0.000	44.594	96.290
50.000	32.400	4.122	0.819	2.028	1.000	44.598	96.290
50.000	32.119	4.122	0.818	1.995	2.000	44.636	96.290

Table 3 Part 2 Pressure Data for p_{sv} , p_{td} , and p_{mm}

p_{sv} (Pa)	p_{td} (Pa)	p_{mm} (Pa)
73.425	69.422	71.239
140.897	136.174	138.992
239.625	234.967	237.382
353.235	348.446	350.219
505.543	500.640	503.409
671.743	666.186	668.306
877.631	873.117	874.801
1089.473	1085.388	1088.021

Table 4 Part 3 Pressure Data for p_{sv} , p_{td} , and p_{mm}

p_{sv} (Pa)	p_{td} (Pa)	p_{mm} (Pa)
65.487	70.757	70.741
63.999	70.757	70.741
58.046	72.092	70.741
127.006	138.844	136.501
136.928	138.844	136.501
134.944	138.844	136.501
210.354	232.297	224.927
225.733	230.962	224.927
225.237	232.297	224.927
304.616	351.116	341.750
331.902	351.116	341.750
327.437	351.116	341.750
431.622	496.635	478.251
473.792	499.305	478.251
462.877	495.300	478.251
567.558	671.526	640.159
618.658	668.856	640.159
615.185	671.526	640.159
724.331	877.122	836.939
797.260	877.122	836.939
788.330	878.457	836.939
910.375	1092.064	1038.701
1006.125	1093.399	1038.701
989.754	1092.064	1038.701

Table 5 Pressure Uncertainty for p_{sv} , p_{td} , and p_{mm}

δp_{sv} (Pa)	δp_{td} (Pa)	δp_{mm} (Pa)
2.481	13.350	1.2454

Table 6 Velocity Data for v_{sv} , v_{td} , and v_{mm}

v_{sv} (m/s)	v_{td} (m/s)	v_{mm} (m/s)
10.927	11.358	11.505
10.802	11.358	11.505
10.287	11.465	11.505
15.217	15.910	15.982
15.800	15.910	15.982
15.685	15.910	15.982
19.584	20.580	20.515
20.287	20.521	20.515
20.265	20.580	20.515
23.567	25.301	25.287
24.599	25.301	25.287
24.433	25.301	25.287
28.052	30.091	29.914
29.391	30.172	29.914
29.050	30.051	29.914
32.168	34.991	34.609
33.585	34.921	34.609
33.491	34.991	34.609
36.340	39.990	39.573
38.126	39.990	39.573
37.912	40.020	39.573
40.741	44.621	44.086
42.830	44.649	44.086
42.480	44.621	44.086

Table 7 Velocity Uncertainty for v_{sv} , v_{td} , and v_{mm}

v_{sv} (m/s)	v_{td} (m/s)	v_{mm} (m/s)
0.0187	0.0195	0.1032
0.0185	0.0195	0.1032
0.0176	0.0197	0.1032
0.0261	0.0273	0.0779
0.0271	0.0273	0.0779
0.0269	0.0273	0.0779
0.0336	0.0353	0.0668
0.0348	0.0352	0.0668
0.0348	0.0353	0.0668
0.0404	0.0434	0.0633
0.0422	0.0434	0.0633
0.0419	0.0434	0.0633
0.0481	0.0516	0.0644
0.0504	0.0518	0.0644
0.0498	0.0515	0.0644
0.0552	0.0600	0.0682
0.0576	0.0599	0.0682
0.0574	0.0600	0.0682
0.0623	0.0686	0.0740
0.0654	0.0686	0.0740
0.0650	0.0686	0.0740
0.0699	0.0765	0.0801
0.0735	0.0766	0.0801
0.0729	0.0765	0.0801

I. Appendix C: MATLAB Code

```
%% Header
% Author: Zakary Steenhoek
% Date: 19 September 2024
% AEE360::LAB01

clc; clear; close all; % Reset

%% Global

% Constants
R_AIR = 287.0; % gas constant [J/kg*K]
MANO_BIAS = abs(-0.048); % manometer bias [inH2O]
ERR_ABS_TRANSDUCER = 100; % machine error [Pa]
ERR_THERMO = 1; % machine error [deg C]
ERR_TRANSDUCER = 0.01; % machine error [Volt]
ERR_SCANNIVALVE = 0.005; % machine error [Volt]
ERR_MANOMETER = 0.005; % machine error [inH2O]
RATIO_A1A2 = 6.25; % dimensionless
RATIO_A2A1 = 1/RATIO_A1A2; % dimensionless

% Measurements
p_measured_kpa = 96.29; % ambient atmospheric pressure [kPa]
p_abs_pa = 96290; % ambient atmospheric pressure [Pa]
t_measured_cel = 32.7; % ambient air temperature [degrees celcius]
t_air_kel = 305.85; % ambient air temperature [Kelvin]

% Symbolic variables
syms P T MM RHO

%% Data

% Import files
allData_2 = importdata("Lab1_ThuB600_2.txt");
allData_3 = importdata("Lab1_ThuB600_3.txt");

% Data needed for pt. 2
manometer_2 = allData_2.data(:, 3); % manometer pressure differential [inH2O]
transducer_2 = allData_2.data(:, 4); % transducer reading [Volts]
scannivalve_2 = abs(allData_2.data(:, 5)); % scannivalve reading [Volts]

% Data needed for pt. 3
hz_3 = allData_3.data(:, 1); % frequency [Hz]
manometer_3 = allData_3.data(:, 3); % manometer pressure differential [inH2O]
transducer_3 = allData_3.data(:, 4); % transducer reading [Volts]
scannivalve_3 = allData_3.data(:, 5); % scannivalve reading [Volts]
velocity_3 = allData_3.data(:, 7); % flow velocity [m/s]

%% Equations & Functions

% Ideal Gas Law -> rearranged for rho
gasLaw_rho = @(P,T) P./(R_AIR*T); % Ideal Gas Law [Pa, deg C]
```



```

% Partial derivatives of RHO -> error calculations
gasLaw_dP = diff(gasLaw_rho(P,T),P);          % ptl rho w.r.t pressure
gasLaw_dT = diff(gasLaw_rho(P,T),T);          % ptl rho w.r.t temp

% Dynamic pressure -> rearranged for velocity
vDyn = @(P,RHO) sqrt((2.*P)./RHO);            % dynamic pressure [Pa, kg/m^3]

% Partial derivatives of Vdyn -> error calculations
vDyn_dP = diff(vDyn(P,RHO),P);                % ptl velocity w.r.t pressure
vDyn_dRHO = diff(vDyn(P,RHO),RHO);            % ptl velocity w.r.t. density

% Bernoulli's Equation -> rearranged with mass conservation
V2 = @(MM,RHO) sqrt((2*MM)./(RHO*(1-RATIO_A2A1^2)));

% Partial derivatives of V2 -> error calculations
V2_dMM = diff(V2(MM,RHO),MM);                % ptl velocity w.r.t pressure differential
V2_dRHO = diff(V2(MM,RHO),RHO);              % ptl velocity w.r.t density

% inH2O to Pa -> from internet
inH2OToPa = @(inH2O) inH2O*249.089;          % pressure conversion

% Mass conservation -> incompressible flow
V1 = @(V2) RATIO_A2A1*V2;                    % velocity conversion

%% Misc

% Convert manometer values from inH2O to Pa & factor in bias
manometer_2 = manometer_2+MANO_BIAS;
manometer_3 = manometer_3+MANO_BIAS;
mm_2 = inH2OToPa(manometer_2);
mm_3 = inH2OToPa(manometer_3);

% Convert manometer machine error to Pa
ERR_MANOMETER_PA = ERR_MANOMETER*249.089;

%% Part 1: Density & Uncertainty

% Air density
rho = gasLaw_rho(p_abs_pa, t_air_kel);

% Air density uncertainty due to machine error
dP_rho = 1/(R_AIR*t_air_kel);
dT_rho = (p_abs_pa)/(R_AIR*t_air_kel^2);
err_rho = sqrt((ERR_ABS_TRANSDUCER*dP_rho).^2+(ERR_THERMO*dT_rho).^2);

%% Part 2: Instrument Calibration

% Manometer reading vs. scannivalve & transducer -> LSQ fit
[coeff_sv_2, S_sv_2] = polyfit(scannivalve_2, mm_2, 1);
[coeff_td_2, S_td_2] = polyfit(transducer_2, mm_2, 1);
m_sv = coeff_sv_2(1); m_td = coeff_td_2(1);
p_sv_2 = m_sv*scannivalve_2;
p_td_2 = m_td*transducer_2;

% Pressure uncertainty due to machine error & R^2

```

```

err_p_sv = m_sv*ERR_SCANNIVALVE;
err_p_td = m_td*ERR_TRANSDUCER;
R_sq_sv_2 = 1 - (S_sv_2.normr/norm(mm_2-mean(mm_2)))^2;
R_sq_td_2 = 1 - (S_td_2.normr/norm(mm_2-mean(mm_2)))^2;

%% Part 3: Wind Tunnel Calibration

% Scannivalve air flow velocity vs. fan speed -> LSQ fit
p_sv = m_sv.*scannivalve_3;
v_sv = vDyn(p_sv, rho);
coeff_v_sv_3 = polyfit(hz_3, v_sv, 1);
v_hz_sv = coeff_v_sv_3(1);

% Scannivalve velocity error
dP_sv = 2^(1/2)/(2*rho*(p_sv/rho).^(1/2));
dRHO_sv = -(2^(1/2)*p_sv)/(2*rho.^2*(p_sv./rho).^(1/2));
err_v_sv = sqrt((err_p_sv*dP_sv).^2+(err_rho*dRHO_sv).^2);

% Transducer air flow velocity vs. fan speed -> LSQ fit
p_td = m_td.*transducer_3;
v_td = vDyn(p_td, rho);
coeff_v_td_3 = polyfit(hz_3, v_td, 1);
v_hz_td = coeff_v_td_3(1);

% Transducer velocity error
dP_td = 2^(1/2)/(2*rho*(p_td./rho).^(1/2));
dRHO_td = -(2^(1/2)*p_td)/(2*rho.^2*(p_td./rho).^(1/2));
err_v_td = sqrt((err_p_td*dP_td).^2+(err_rho*dRHO_td).^2);

% Manometer air flow velocity vs. fan speed -> LSQ fit
v2_ca = V2(mm_3,rho); v1_ca = V1(v2_ca);
coeff_v_ca = polyfit(hz_3, v2_ca, 1);
v_hz_ca = coeff_v_ca(1);

% Manometer velocity error
dMM_ca = 625./(609*rho*((1250*mm_3)/(609*rho)).^(1/2));
dRHO_ca = -(625*mm_3)/(609*rho.^2*((1250*mm_3)/(609*rho)).^(1/2));
err_v_ca = sqrt((ERR_MANOMETER_PA*dMM_ca).^2+(err_rho*dRHO_ca).^2);

% True air flow velocity vs. fan speed -> LSQ fit
coeff_v_real = polyfit(hz_3, velocity_3, 1);
v_hz_real = coeff_v_real(1);

%% Plots

% Figure 1 config
figure(1); % tiledlayout(2,1);

% Manometer reading vs. scannivalve reading
%sv_2 = nexttile;
hold on; grid on;
fplot(poly2sym(coeff_sv_2), 'k-');
errorbar(scannivalve_2, mm_2, err_p_sv, 'k. ');
title('Manometer Pressure (Pa) vs. Absolute Scannivalve Voltage (|E|)');
xlabel('Volts (|E|)'); ylabel('Pressure (Pa)');
legend('Conversion factor (V -> Pa)', 'Pressure uncertainty', ...

```

```

    'Location', 'southeast'); %fontsize('scale', 1.5);
xlim([0,2.25]); ylim([-150,1300]);
hold off;

% Manometer reading vs. transducer reading
%td_2 = nexttile;
figure(2); hold on; grid on;
fplot(poly2sym(coeff_td_2), 'k-');
errorbar(transducer_2, mm_2, err_p_td, 'k. ');
title('Manometer Pressure (Pa) vs. Transducer Voltage (E)');
xlabel('Volts (E)'); ylabel('Pressure (Pa)');
legend('Conversion factor (V -> Pa)', 'Pressure uncertainty', ...
    'Location', 'southeast'); %fontsize('scale', 1.5);
xlim([0,0.83]); ylim([-150,1300]);
hold off;

% Figure 2 config
figure(3); % tiledlayout(3,1);

% Scannivalve velocity vs. fan speed
%sv_3 = nexttile;
grid on; hold on;
fplot(poly2sym(coeff_v_sv_3), 'k-');
errorbar(hz_3, v_sv, err_v_sv, 'k. ');
title('Scannivalve Velocity (m/s) vs. Fan Speed (Hz)');
xlabel('Fan Speed (Hz)'); ylabel('Velocity (m/s)');
legend('Flow velocity', 'Velocity Uncertainty', ...
    'Location', 'southeast'); %fontsize('scale', 1.5);
xlim([13,52]); ylim([0,60]); hold off;

% Transducer velocity vs. fan speed
%td_3 = nexttile;
figure(4); grid on; hold on;
fplot(poly2sym(coeff_v_td_3), 'k-');
errorbar(hz_3, v_td, err_v_td, 'k. ');
title('Transducer Velocity (m/s) vs. Fan Speed (Hz)');
xlabel('Fan Speed (Hz)'); ylabel('Velocity (m/s)');
legend('Flow velocity', 'Velocity Uncertainty', ...
    'Location', 'southeast'); %fontsize('scale', 1.5);
xlim([13,52]); ylim([0,60]); hold off;

% Manometer velocity vs. fan speed
%ca_3 = nexttile;
figure(5); grid on; hold on;
fplot(poly2sym(coeff_v_ca), 'k-');
errorbar(hz_3, v2_ca, err_v_ca, 'k. ');
title('Manometer Velocity (m/s) vs. Fan Speed (Hz)');
xlabel('Fan Speed (Hz)'); ylabel('Velocity (m/s)');
legend('Flow velocity', 'Velocity Uncertainty', ...
    'Location', 'southeast'); %fontsize('scale', 1.5);
xlim([13,52]); ylim([0,60]); hold off;

% Velocity from all three instruments against true velocity
figure(6); grid on; hold on;
fplot(poly2sym(coeff_v_real), 'k--', 'LineWidth', 2);
fplot(poly2sym(coeff_v_sv_3), 'k-', 'LineWidth', 1);

```

```

fplot(poly2sym(coeff_v_td_3), 'b.-', 'LineWidth',1);
fplot(poly2sym(coeff_v_ca), 'r.-', 'LineWidth',1);
title('Flow Velocity (m/s) vs. Fan Speed (Hz)');
xlabel('Fan Speed (Hz)'); ylabel('Velocity (m/s)');
legend('True velocity', 'Scannivalve velocity', ...
    'Transducer velocity', 'Manometer velocity', ...
    'Location', 'southeast'); %fontsize('scale', 1.5);
xlim([13,52]); ylim([0,60]); hold off;

```

VI. Acknowledgements

I would first like to thank my lab TA for the beautiful figures and guidance throughout the experiment. I would also like to thank Monster Beverage Corporation for providing me with the necessary caffeine to get through this week. Lastly I would like to thank my cat Robby for the moral support he provided, i.e. screaming outside my door whenever I did not let him watch me do my homework and step on my keyboard.

References

- [1] NASA, “Low speed tunnel operation,” , 2021. URL <https://www.grc.nasa.gov/www/k-12/airplane/tunop.html>.
- [2] Craig, B., “What is absolute pressure transmitter [and] how does it work?” , Jul 2023. URL <https://www.transmittershop.com/blog/absolute-pressure-transmitter-working-principle-applications/#:~:text=Simply%2C%20the%20side%20of%20the,mechanical%20energy%20into%20electrical%20signals>.
- [3] munroscientificdivision, 2024. URL <https://www.munroscientific.co.uk/a-guide-for-laboratory-thermometer#:~:text=A%20laboratory%20thermometer%20is%20an,scale%20that%20indicates%20the%20temperature.>
- [4] click2electro, “Manometer Basics & Micromanometer,” , Apr 2023. URL <https://click2electro.com/forum/instrumentation-measurement/manometer-basics-micromanometer/>.
- [5] links open overlay panelGiuseppe P. Russo, A., and chapter highlights pressure sensors ranging from the classical manometers, A., “Pressure sensors,” , Mar 2014. URL <https://www.sciencedirect.com/science/article/pii/B9781845699925500012>.
- [6] NASA, “Pitot tube,” , 2024. URL <https://www.grc.nasa.gov/www/k-12/VirtualAero/BottleRocket/airplane/pitot.html>.
- [7] www.convertunits.com, “Convert inH2O to pascal,” , 2024. URL <https://www.convertunits.com/from/inH20/to/pascal>.
- [8] ThuB600, “Lab1_ThuB600_2,” , 2024. URL https://canvas.asu.edu/courses/200674/files/91877142?module_item_id=14711061.
- [9] ThuB600, “Lab1_ThuB600_3,” , 2024. URL https://canvas.asu.edu/courses/200674/files/91877141?module_item_id=14711060.
- [10] CalculatorSoup, L., “Celsius to Kelvin: °C to K,” , Aug 2023. URL <https://www.calculatorsoup.com/calculators/conversions/celsius-to-kelvin.php>.